New porphyrin dendrimers with fluorenyl-based connectors: a simple way to improving the optical properties over dendrimers featuring 1,3,5-phenylene connectors

Xu Zhang, Sarra Ben Hassine, Nicolas Richy, Olivier Mongin, Mireille Blanchard-Desce, Frédéric Paul, Christine Paul-Roth

New Porphyrin Dendrimers with Fluorenyl-based Connectors: A Simple Way to improving the Optical Properties over Dendrimers featuring 1,3,5-Phenylene Connectors

Xu Zhang,[a] Sarra Ben Hassine,[a,b] Nicolas Richy,[a] Olivier Mongin,[a] Mireille Blanchard-Desce,[c] Frédéric Paul,[a] Christine O. Paul-Roth,[a,*]

[a] *Univ Rennes, INSA Rennes, CNRS, ISCR (Institut des Sciences Chimiques de Rennes) – UMR 6226, F-35000 Rennes, France.*

[b] *Faculté des Sciences de Tunis, Université de Tunis El Manar, Tunisie*

[c] *Univ. Bordeaux, Institut des Sciences Moléculaires (CNRS UMR 5255), 33405 Talence, France*

*Corresponding author: christine.paul@univ-rennes1.fr or christine.paul@insa-rennes.fr

tel : (+33) (0) 2 23 23 63 72 fax: (+33) (0) 2 23 23 63 72

TOC Figure

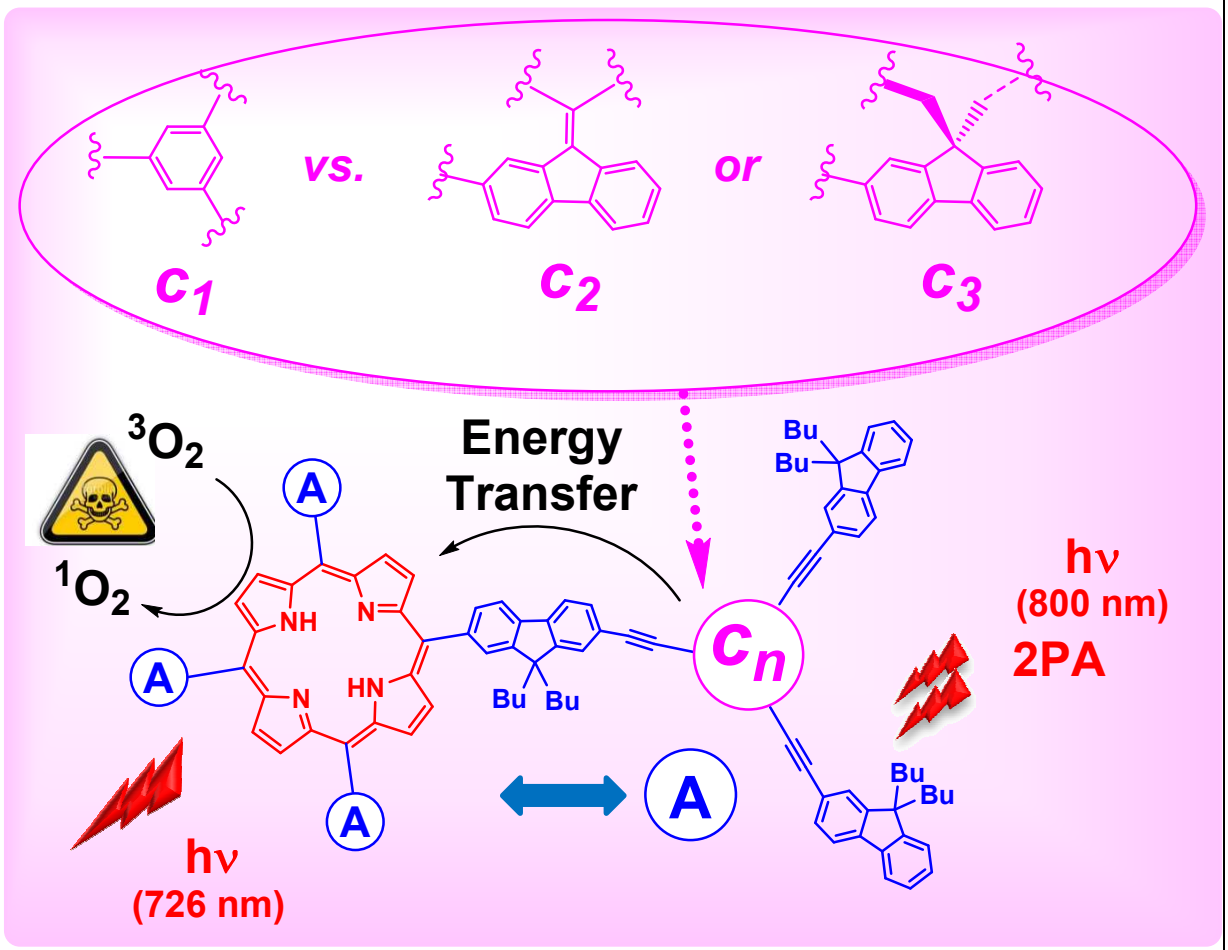

Electronic Supplementary Information (ESI) available: [details of any supplementary information available should be included here]. See DOI: 10.1039/x0xx00000x

Abstract: Two new *meso*-tetrafluorenylporphyrin-cored dendrimers **1** and **2** have been synthesized and characterized. The peripheral fluorenyl units of these dendrimers are linked to the central tetrafluorenylporphyrin (**TFP**) core by original **fluorene-based connectors** instead of the more classic 1,3,5-phenylene unit. Selected linear and non-linear optical (LO and NLO) properties were determined for these dendrimers *via* absorption or emission studies and by two-photon excited fluorescence (TPEF) measurements. Dendrimer **1**, which has a conjugated and quite rigid structure, exhibits a significantly higher two-photon absorption (2PA) cross-section than dendrimer **2**, presenting a non-conjugated and more flexible structure, as well as better luminescence and singlet oxygen activation quantum yields. Both dendrimers exhibit higher 2PA cross-sections than several closely related **TFP**-based dendrimers previously characterized. However, among them, dendrimer **1** is the only one outperforming all these compounds in terms of 2PA brightness and 2PA oxygen sensitization. Thus, the new type of connector (or dendrimeric node) introduced in **1** appears quite appealing for the design photosensitizers aimed at theranostic uses in the future.

Keywords
Porphyrin * fluorene * fluorescence * energy transfer * dendrimer *node

Introduction

Stimulated by their remarkable photochemical and redox properties which can be fine-tuned by modification of the peripheral substituents, porphyrin-based systems are foreseen as key building blocks for many applied developments nowadays. In this respect, impressive fundamental research based on porphyrins has been undertaken in fields related to material sciences and information treatment these last decades,[1, 2] but also in fields related to health, such as photodynamic therapy (PDT) for instance.[3]

In this particular field, their use for PDT has been revived subsequent to the observation that oxygen sensitization might advantageously be triggered by two-photon absorption (2PA-PDT),[4] especially when the photosensitizers can be coupled to fluorescent probes, allowing to perform curing and imaging at the same time in a so-called theranostic approach.[5, 6] Given that tetraphenylporphyrin (**TPP** in Scheme 1) or related derivatives are only modestly fluorescent in their free base form and presents a rather weak two-photon

absorption cross-section, most of the investigations in this field relied on porphyrin conjugates featuring an expanded π-manifold, in order to enhance the 2PA cross-section and also, to some extent, their fluorescence.[7] However, this expansion was often performed *via* alkynyl or alkenyl linkers appended at their *meso*-positions.[4, 7] As such, it was usually accompanied by a red-shift of the porphyrin absorptions at lowest energy, reducing thereby the spectral window available to perform two-photon excitation in a wavelength range devoid of linear absorption, an important condition to fully benefit from the advantages of two-photon excitation.

At difference with such approaches, we could recently show with various families of star-shaped[8-10] or dendrimeric porphyrins,[11, 12] that by appending **fluorene-containing dendrons** at the periphery of a central tetra-arylporphyrin core, fluorescent photosensitizers with significantly enlarged one-photon brightnesses could be obtained upon increasing the dendrimer generation. Furthermore, when fully unsaturated dendrons were used such as in $\mathbf{A_n}$ and $\mathbf{B_n}$ (Scheme 1),[11, 12] a significant increase in the two-photon absorption cross-section of these photosensitizers could be achieved *without* diminishing the optical window for excitation.[11, 12] This remarkable property most likely results from the partial disruption of the π-manifold (taking place at the *meso* positions in the most stable conformers). Furthermore, these twisted conformations adopted by the *meso* aryl groups allow the peripheral dendrons to behave as efficient light-harvesting *antennae*, while preserving quite sizeable efficiencies for two-photon oxygen sensitization at the porphyrin core. This is plainly shown by the relevant figure of merit (δ_{O2}) given for several of these compounds in Scheme 1, revealing that among the members of the two dendrimer families $\mathbf{A_n}$ and $\mathbf{B_n}$ represented, the **TFP**-cored dendrimers ($\mathbf{B_n}$) are always the most efficient photosensitizers for oxygen.[13] The δ_{O2} factor corresponds to the 2PA singlet oxygen production for a given compound ($\Phi_{\Delta}\bullet\sigma_2^{max}$) normalized by that of **TPP**. Furthermore, since the luminescence quantum yield (Φ_{fl}) of the central porphyrin is usually preserved,[11] the one-photon brightness improves with successive generations in a given family.

However, in contrast to the one-photon brightness, the two-photon brightness and two-photon photosensitization (or δ_{O2} factor) decrease with increasing dendrimer generations in

each of these dendrimer families.[11, 12] This decrease can be traced back to the weak electronic communication operative between fluorenyl units through the *meta*-positions of the 1,3,5-phenylene units used as dendrimeric nodes. As a result, the two-photon absorption cross-section (σ_2) does not scale anymore with the number of fluorenyl units present in the peripheral dendrons, presently making the smallest derivatives in each family (**A_0** and **B_0**) the most promising two-photon photosensitizers for any applied development. Also possibly in line with this poor electronic communication, the energy transfer from the periphery to the central porphyrin does no more take place quantitatively in the generation two dendrimer **B_2**.[11]

In order to improve further these photosensitizers in their higher generations, we decided to test another node and to replace the classic **1,3,5-phenylene unit** (***C_1***; Scheme 2) by the new **fluorenyl-based unit** (***C_2***) in the dendrons. Thus, new **TFP**-based dendrimer **1**, the analogue of dendrimer **B_1** featuring these new connectors, was targeted. Likewise to **B_1**, *n*-butyl groups were added in position 9 on the terminal fluorene groups to improve the overall solubility of the dendrimer. In *generation one* (G1) dendrimer **1**, contrary to what is happening with classic connector ***C_1***, the 2-alkynylfluorenyl units on ***C_2*** are no more connected to topologically orthogonal positions[14] and a better electronic communication between the various fluorenyl subunits should result. This should positively impact σ_2 in **1**, and in turn, also positively impact the two-photon brightness and the δ_{O2} figure of this compound. Then, in order to make sure that any improvement of these features is not simply related to the increase in the number of fluorene units within each dendron (given that the connector ***C_2*** is also a fluorenyl unit), we also targeted the dendrimer **2** featuring ***c_3*** connections in place of ***C_2***. Likewise to dendrimer **1**, dendrimer **2** has four fluorenyl units in each peripheral dendron, but without any conjugation between three of them. Thus, comparison between **1** and **2** should allow us to evidence the importance of electronic conjugation within the dendrons. The ***C_2*** connector, substituted in the position 9 by a double bond linked to two (2-ethynyl)fluorenyl groups, allows electronic conjugation between the four fluorenyl groups. In contrast, the connector ***C_3***, with a tetrahedral carbon in the position 9 featuring saturated extensions on opposite sides of the central fluorene group does not allow

electronic conjugation with the two pendant fluorene groups. The dendrons in **1**, with rigid and entirely planar *termini* (except for the four butyl chains), will possibly adopt a propeller-shaped conformation around the porphyrin core, while the dendrons in **2**, more flexible, should adopt a more compact three dimensional structure.

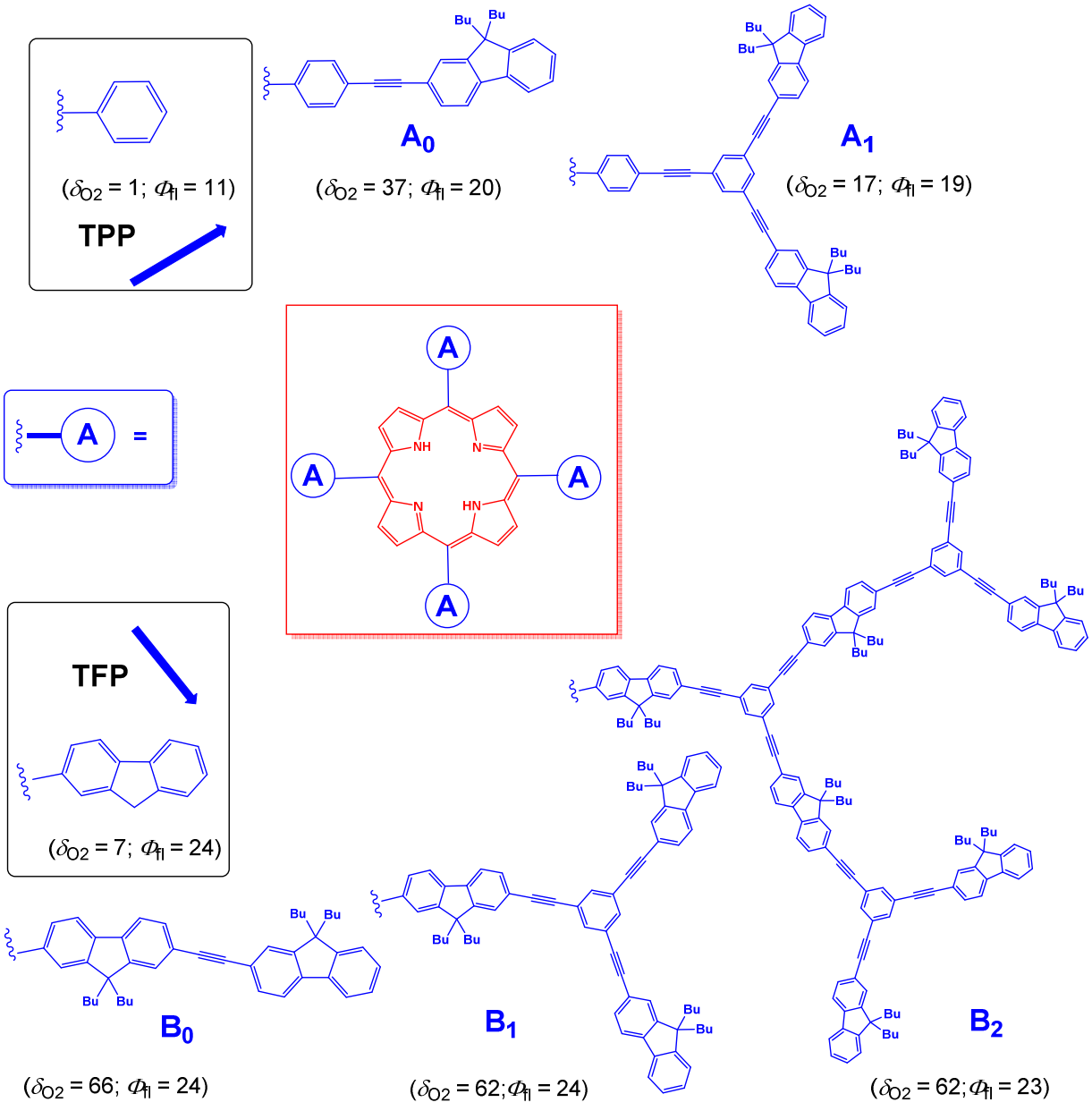

Scheme 1. Selected representatives among two families of tetraarylporphyrin-based dendrimers ($\mathbf{A_n}$ and $\mathbf{B_n}$) along with the reference compounds **TPP** and **TFP**. A figure of merit for two-photon oxygen sensitization (δ_{O2}) measured in CH_2Cl_2 and their fluorescence quantum yields (Φ_{fl}) measured in toluene are given in parenthesis.

Finally, we will also study compounds **4** and **5**, modelizing the new terminal units in **1** and **2**, respectively. These model compounds should help us understanding better some of the photophysical properties of the new dendrimers **1** and **2**, in particular the energy transfer (ET) taking place from peripheral light-harvesting *antennae* toward the central macrocycle. The central core of these dendrimers being modelized by the known tetrafluorenylporphyrin **TFPBu**.[11]

In the following, we will now describe (i) the synthesis of the various model compounds **4**-**5**; (ii) the synthesis and characterization of the targeted **TFP**-based dendrimers **1** and **2** featuring these units as components and (iii) the study of the linear and nonlinear optical properties, as well as their capability to photosensitize oxygen. Their optical properties, energy transfer behavior and two photon absorption properties as well as their singlet oxygen photosensitizing properties will then be compared with those of dendrimer $\mathbf{B_1}$ and discussed in the light of previous results.[11, 12]

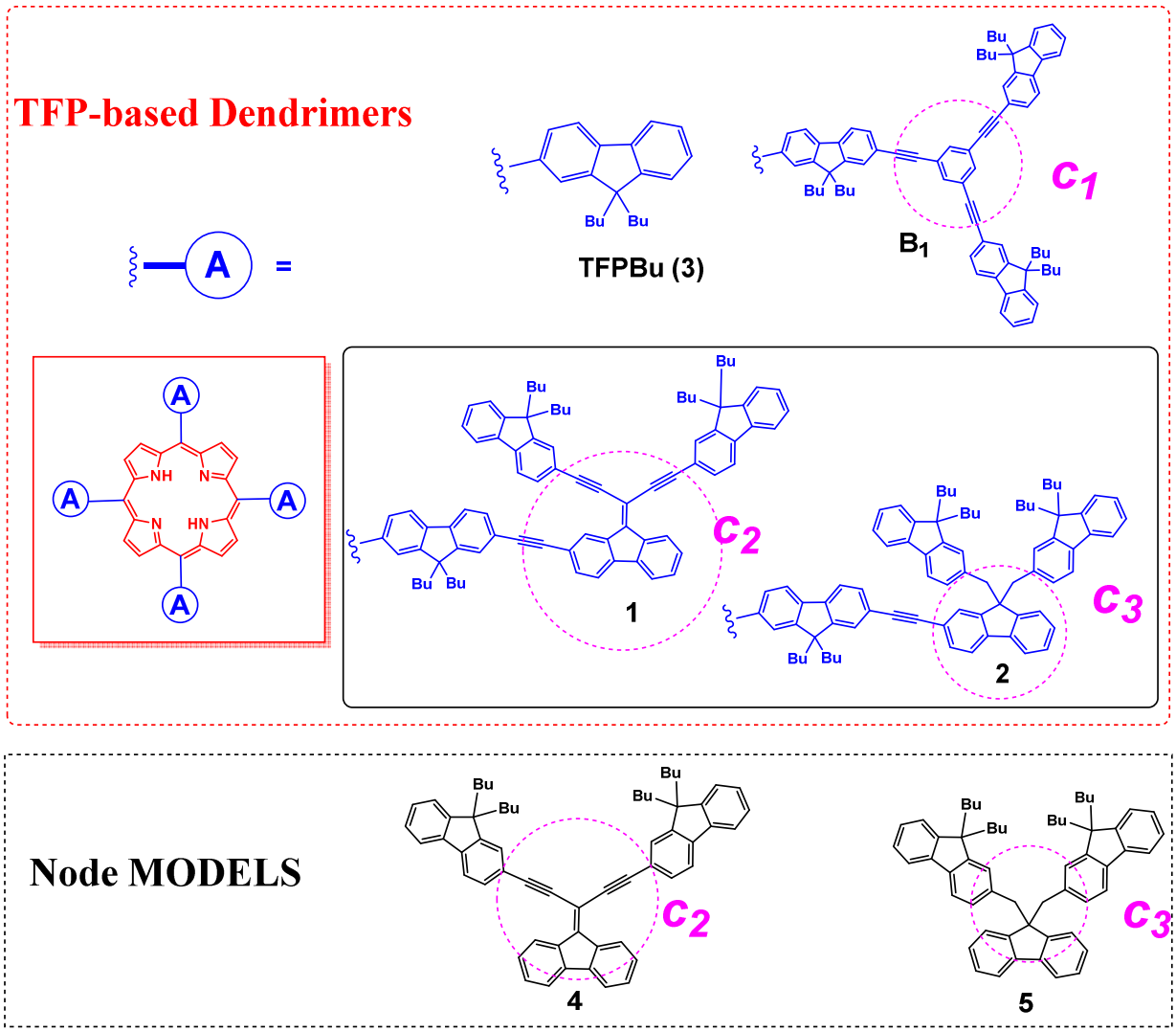

Scheme 2. The known first generation dendrimer $\mathbf{B_1}$ and the targeted analogues **1** and **2**, along with the corresponding **TFP** "core" model **TFPBu** and targeted model compounds **4** and **5**.

Results and discussion

To synthetically access the new dendrimers **1** and **2**, a strategy in three steps was used (Scheme 3), *i.e.* (i) the synthesis of the bromo-terminated dendrons precursors **6** and **7**, (ii) the synthesis of the tetra((7-ethynyl)fluoren-2-yl)porphyrin (**8**), standing for **TFP**-cored precursor, by the Lindsey method,[15, 16] and finally, (iii) the connection of porphyrin **8** to the dendron precursors by Sonogashira coupling reactions.[17] During parts (i) and (ii), the previously discussed model compounds **4** and **5** will also be isolated.

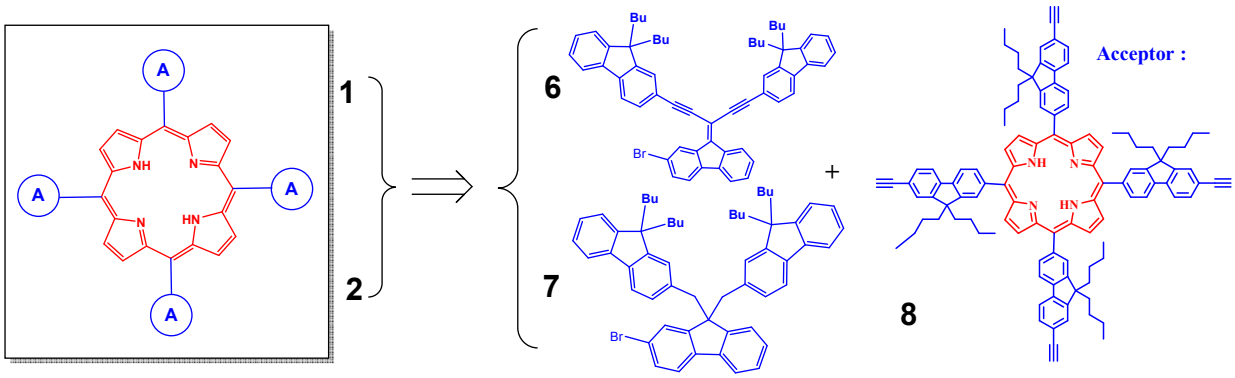

Scheme 3. Proposed retrosynthetic approach followed to access **1** and **2**.

Dendron synthesis

Model Compound 4 and Conjugated Dendron Precursor 6. These molecules were obtained from commercial fluorenone (**9**) in a few steps (Scheme 4).

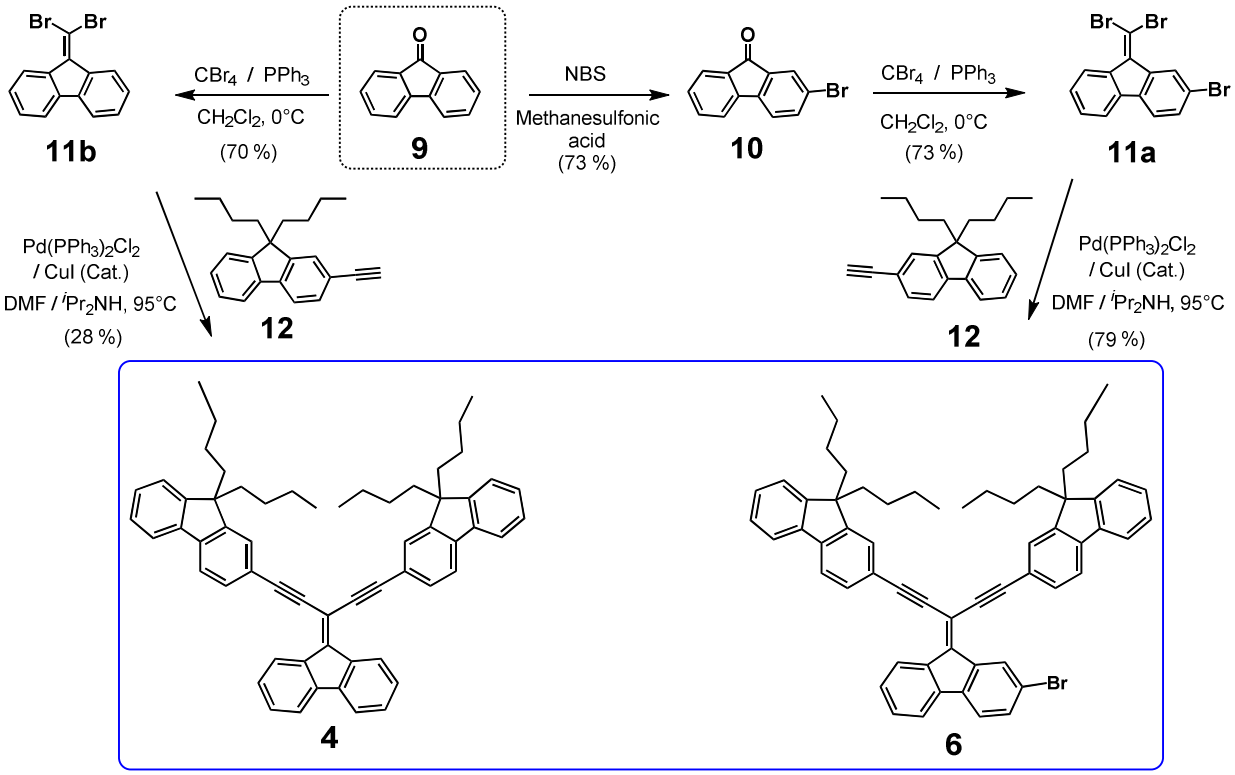

Scheme 4. Syntheses of the conjugated dendron precursor **6** and of the corresponding model compound **4**.

Treatment with *N*-bromosuccinimide (NBS) afforded 2-bromofluorenone (**10**) and further reaction with the *in situ* formed dibromomethylene phosphorane afforded the *gem*-dibromo derivative **11a**. The latter reacted with two equivalents of the terminal alkyne **12**[18, 19] to yield the desired precursor **6** in 42% global yield from **9**. In a similar approach, the model compound **4** was obtained via the intermediate **11b**, albeit in a lower global yield (20%).

We observe by ^{1}H NMR, that exchanging oxygen for a CBr_2 group causes a large shift in the peaks of these protons to low field from 7.6 to 8.6 ppm (see Fig. S1; ESI). In the model compound **4,** bearing two fluorenyl *antennae* in place of the bromine atoms, a further shift to lower field (8.8 ppm) takes place for this doublet. In non-symmetric compounds such as bromo intermediate **11a** or Dendron **6**, the doublet splits, giving a singlet and doublet at low field (Figure 1). This peculiar ^{1}H NMR signal will therefore be used to assess the presence of dendrons like **4** in dendrimer **1**.

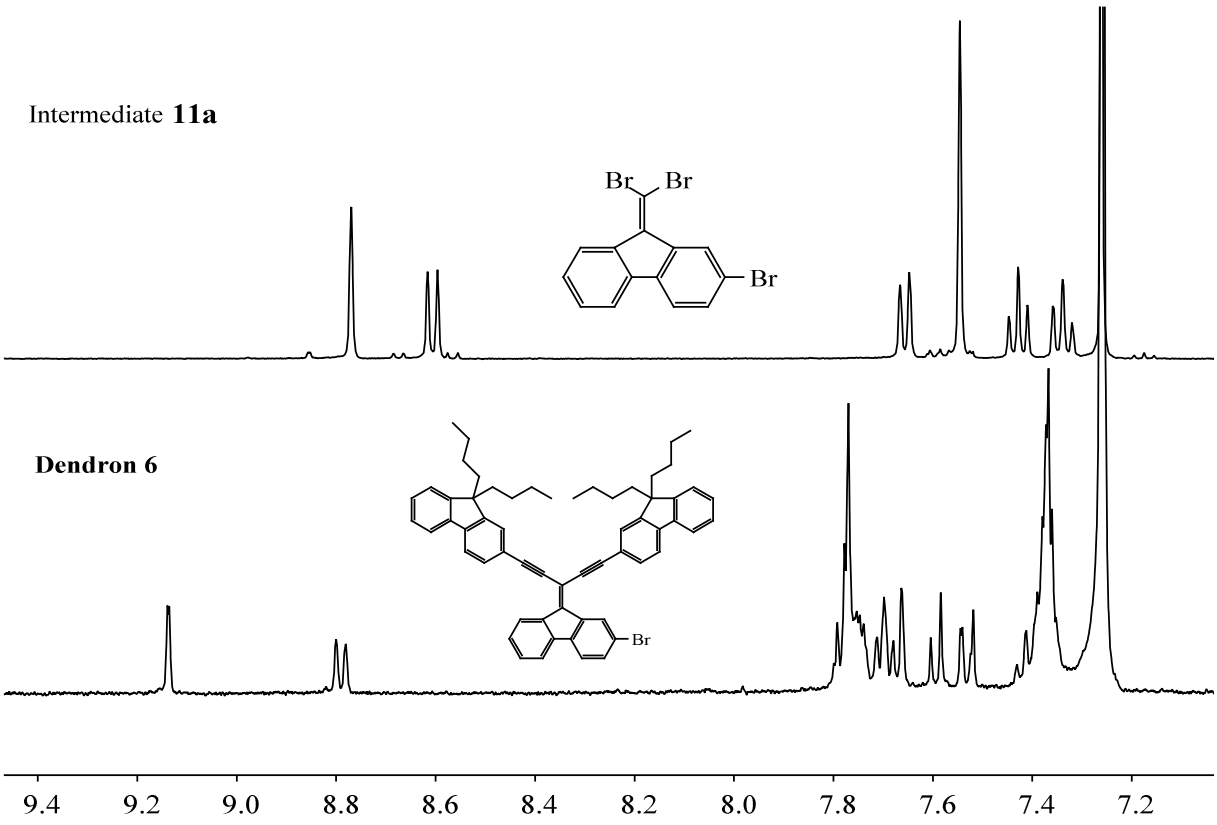

Figure 1. Partial ^{1}H NMR spectra of the intermediate **11a** and of the corresponding dendron precursor **6** in $CDCl_3$.

Model Compound 5 and Non-Conjugated Dendron Precursor 7. These molecules were obtained from commercial 2-bromo-9,9-dibutyl-fluorene (**13**).[11, 12] The latter molecule, after reaction with *n*-BuLi in THF, followed by addition of DMF (Scheme 5), affords the corresponding fluorene carboxaldehyde intermediate (**14**). This compound is subsequently reduced in alcohol and brominated, giving **16** in two steps with 82% overall yield. Different reagents were tested for the bromination of **15**, *i.e.* CBr_4, HBr and NBS,[9, 10, 20, 21] with yields of 31%, 60% and 86% respectively, but NBS turned out to be the most efficient reagent. Finally, the model compound **5** and the desired dendron precursor **7**, were obtained from **16** after reaction with the commercially available synthons **17a** and **17b**, respectively. Notably, **7** could not be isolated using the classical method (*i.e.* Bu_4NBr in toluene) and toluene had to be replaced by DMSO to lead to the desired molecule in a good global yield (59%) from **13**.[22, 23] Likewise, the model compound **5** was isolated in 60% overall yield from **13** by a similar reaction sequence.

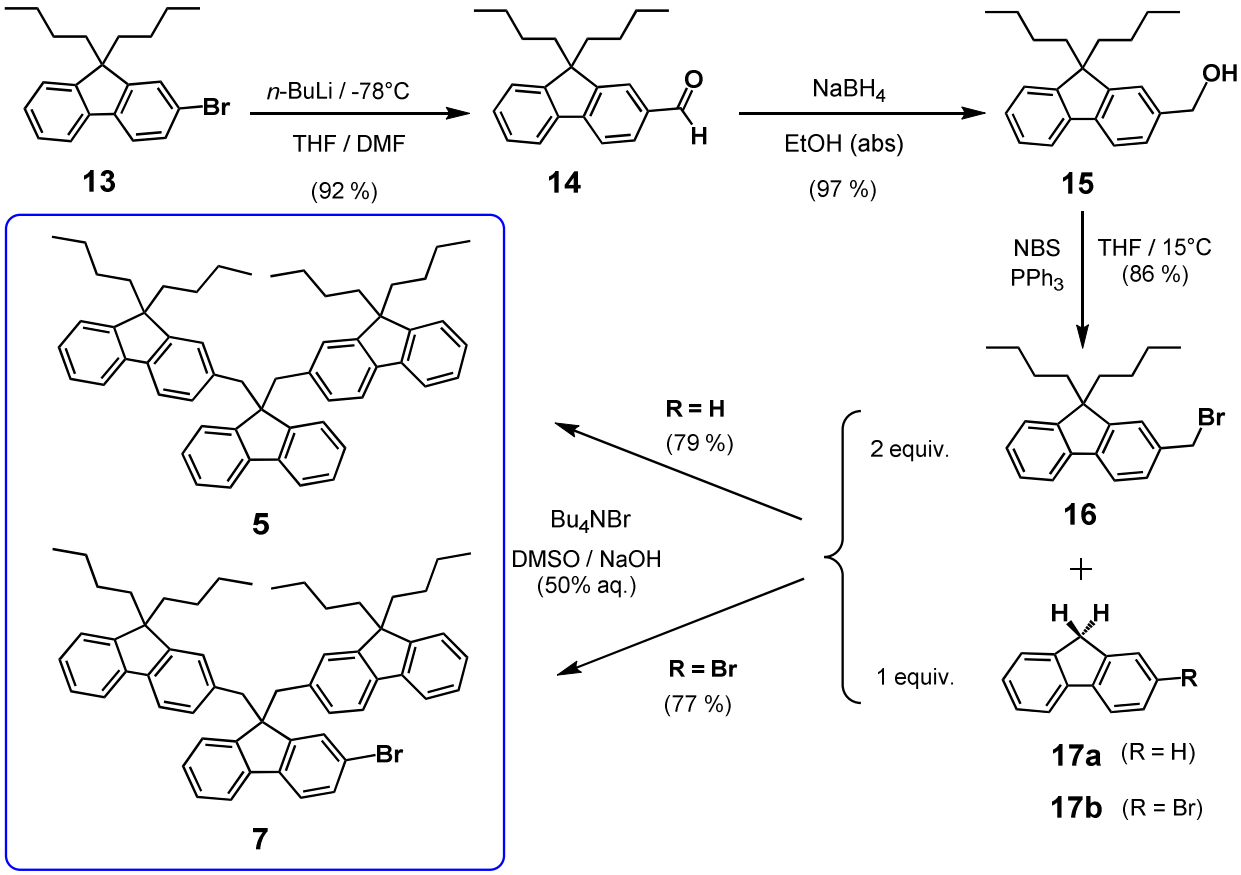

Scheme 5. Syntheses of the non-conjugated dendron precursor **7** and of the corresponding model compound **5**.

In contrast to what had been stated for the derivatives discussed previously, no particular ^{1}H NMR signature could be identified among the aromatic protons of the non-conjugated dendrons. However, the protons of the methylene bridges ($H_{b,b'}$) can now be used as convenient NMR markers (singlet around 3.5 ppm) of dendron such as **5**, providing a simple spectroscopic mean of monitoring the di-substitution at the position 9 of the central fluorenyl unit (see Fig. S2; ESI). Furthermore, this signal is also sensitive to the substitution at the position 2 of the central fluorene, since after introducing the bromo substituent in the 2 position of this fluorene ~~to obtain~~, this singlet in **5** splits into a well-defined AB multiplet (ranging from 3.4 to 3.6 ppm) in dendron **7**.

Porphyrin Synthesis

Synthesis of the TFP Precursor 8. The synthesis of this porphyrin is obtained following Lindsey method (Scheme 6).[15, 16] The aldehyde **18**[24] was condensed with pyrrole to obtain trimethylsilyl (TMS)-protected porphyrin (**19**) and then, compound **19** was readily deprotected, providing the desired tetra-alkynyl precursor **8** in 28% yield from **18**.

Synthesis of Dendrimers 1 and 2. The targeted dendrimers **1** and **2** were then obtained by coupling deprotected porphyrin **8** with the dendrons **6** and **7**, under Sonogashira conditions,[17] these two dendrimers were obtained as dark red solids in 22% (**1**) and 29% (**2**) yields, respectively (Scheme 6). These new dendrimers were characterized by NMR, elemental analysis and MALDI MS for **1**. In ^{1}H NMR (see ESI), the large single peak detected around 9 ppm which corresponds to the eight equivalent β-pyrrolic protons of the **TFP** core is diagnostic of the symmetric structure of these dendrimers. Furthermore, for dendrimer **1**, we can recognize the eight diagnostic protons (H_1 and H_8) corresponding to the dendron as a singlet and doublet at high field (8.97 and 8.87 ppm), while for dendrimer **2**, a large but unresolved signal around 3.6 ppm, corresponding to the sixteen protons of the bridging methylene units of the peripheral dendrons is observed in addition to the eight equivalent β-pyrrolic protons of the **TFP** core (see ESI).

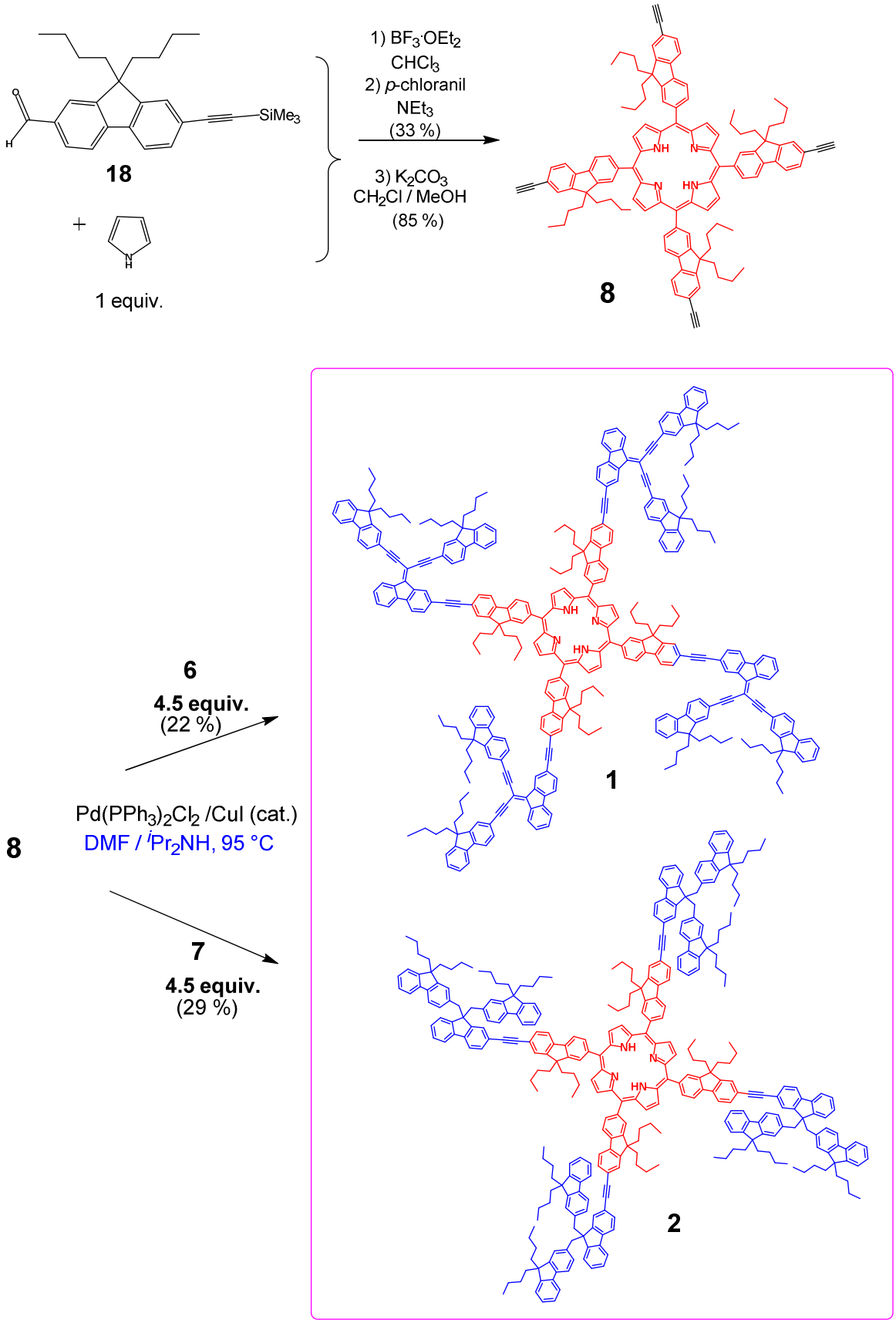

Scheme 6. Synthesis of the generation one (G1) **TFP**-cored dendrimers **1** and **2**.

Photophysical properties

The normalized UV-visible (abs) and emission (em) spectra of the porphyrins **1**, **2**, of the precursor porphyrin **TFPBu** (compound **3**; without the extra dendrons) and of the node models **4**, **5** (Scheme 2) were measured in CH_2Cl_2 at room temperature (Figures 2-4) and compared to those of the known dendrimers $\mathbf{B_1}$ and $\mathbf{B_0}$ (Scheme 1). Whereas the former compound corresponds to the best 2PA photosensitizer among the various first generation dendrimers characterized by our group, so far, the latter compound corresponds to the lead compound in this respect. Furthermore, $\mathbf{B_0}$ shares also the same extended central **TFP** platform with dendrimers **1** and **2**.

Absorption spectra

The new dendrimers **1** and **2** have several characteristic features in their UV-visible absorption spectra (Figure 2): (i) an intense Soret-band around 430 nm and four Q-bands from 520-650 nm, which are typical for free base porphyrin absorptions[25, 26] and (ii) an extra absorption, around 300-400 nm, which corresponds to a $\pi^* \leftarrow \pi$ transition of the conjugated dendrons.[27] This absorption, largely fluorenyl-based, is absent for the model porphyrin **TFPBu (3)**, suggesting that the *unconjugated meso*-fluorenyl groups of this compound absorb below 290 nm,[28-29] whereas the absorption band of the *meso*-ethynylfluorenyl groups of precursor **8** is slightly red-shifted and appears at 292 nm. Those of **1** and **2**, which have *meso*-fluorenylethynylfluorenyl groups, are even more red-shifted (330-350 nm) and more intense, likewise to what had been previously observed with $\mathbf{B_0}$ and $\mathbf{B_1}$.[11]

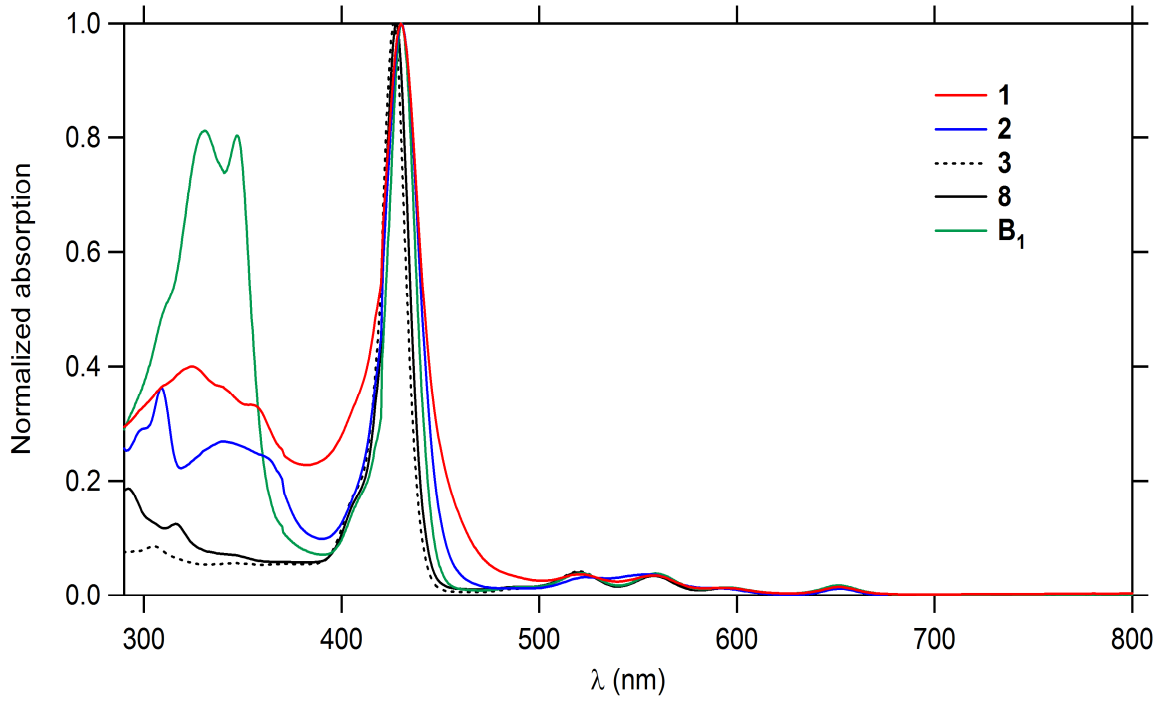

Figure 2. Normalized UV-visible (abs) spectra of new conjugated dendrimers **1**, **2** and reference compounds **3**, **8** and $\mathbf{B_1}$ in CH_2Cl_2.

After normalizing the spectra on the intensity of the Soret-band (Figure 2), it is clear that the porphyrin-based transitions (Soret-band and Q-bands) do not show any significant shifts and that the Q-bands remain of almost constant intensity. Thus, in comparison to $\mathbf{B_0}$ or $\mathbf{B_1}$, the new fluorenyl-based connector present in **1** or **2** does not appear to reduce the transparency window in which these dendrimers can undergo selective two-photon excitation (*i.e.* the frequency range devoid of linear absorption).

Table 1. Photophysical data of new dendrimers **1**, **2** and bare porphyrin **8**, of the model compounds **TFPBu (3), 4, 5**, reference **TPP** and of the known dendrimers $\mathbf{B_0}$ and $\mathbf{B_1}$ in CH_2Cl_2 at R.T.

	UV-visible absorption [a] **/nm**			**Emission** [a] **/nm**			
	Ligand-based Absoption	Soret Band	Q-Bands	λ_{ex}	λ_{em}	Φ_{fl} [b] (%)	**Refs**
1	**325**	**430**	**521, 557, 593, 652**	**660**	**726**	**17**	**This work**
2	**309, 341**	**430**	**524, 555, 591, 652**	**660**	**725**	**12**	**This work**

TFPBu(3)	/	426	519, 555, 592, 652	660	724	18	This work
4	275, 323, 410	/	/	410	469	0.2	This work
5	274, 308	/	/	273	312	59	This work
8	292	428	520, 558, 594, 652	660	724	19	This work
TPP	-	417	513, 548, 589, 646	653	721	11	[11]
$\mathbf{B_0}$	341	432	522, 559, 594, 652	660	726	23	This work
$\mathbf{B_1}$	333	431	520, 557, 597, 652	660	725	22	This work

[a] Experiments were performed in CH_2Cl_2 (HPLC grade): Excitation (λ_{ex}) and emission (λ_{em}) wavelength maximas.

[b] Fluorescence quantum yields were measured in CH_2Cl_2 (HPLC grade) using $\mathbf{H_2TPP}$ (Φ_{fl} = 11%) as standard in toluene, upon excitation at the Soret band.

[c] For values in toluene, see ref. [11].

It should be noted that the Soret bands of **1** and **2** are broader than those of **TFPBu (3)** and **8**, presumably in relation with the extension of the π-manifold after appending the peripheral dendrons, recalling the broadening previously observed for $\mathbf{B_0}$ or $\mathbf{B_1}$. This broadening is even more evident in the case of dendrimer **1**, in which the central porphyrin and peripheral dendrons are fully conjugated. Deeper in the UV region, $\mathbf{B_0}$ exhibits a broad and intense absorption band which maximum appears at 341 nm (*vs.* 333 nm for $\mathbf{B_1}$), corresponding to the absorption of the four conjugated *meso*-fluorenyl ethynylfluorenyl groups. Dendrimer **2**, which possesses a nearly similar set of conjugated groups at its *meso* positions, also exhibit a very similar absorption band with a maximum at the same wavelength, but along with another sharper band at 309 nm, which can therefore be attributed to the eight non-conjugated fluorenes of the flexible *antennae*. In Dendrimer **1**, these two bands seem to overlap, resulting in an even stronger and broader band with a maximum at 325 nm, *i.e.* at an intermediate value between those of Dendrimer **2**. This change can now be related to the extra-conjugation operative between the rigid *antennae* and the *meso*-fluorenyl ethynylfluorenyl groups.

Emission spectra

Upon excitation in their Soret-band, the Dendrimers **1**, **2** and the reference compounds **TFPBu**, **8** exhibit a strong red emission, with characteristic porphyrin peaks Q(0,0) and Q(0,1).[30] After normalizing the emission intensities of these compounds on their Q(0,0) peaks, they exhibit very similar emission spectra, *i.e.* a strong Q(0,0) band and a weaker Q(0,1) band at the same wavelengths (Figure 3). However, the intensity ratios between Q(0,0) and Q(0,1) are slightly more different for extended compounds **1** and **2** than for shorter ones **TFPBu** and **8**.

In contrast, the fluorescence quantum yields are much more impacted by the structural modifications, even if all these tetrafluorenylporphyrins exhibit higher values than **TPP** (Table 1). The quantum yield increases from 11% up to 18 or 19% upon extension of the **TFP** platform, *i.e.* when going to **TFPBu** (fluorene) or **8** (ethynylfluorene). Both dendrimers **1** and **2**, in which *antennae* are replacing on the peripheral fluorenyls the butyl chains of $\mathbf{B_0}$, exhibit lower fluorescence quantum yields (17% and 12%, respectively) than $\mathbf{B_0}$ (23%). They also fluoresce less than the *generation 1* dendrimer $\mathbf{B_1}$ (22%). This behavior can probably be explained by an increase of the internal conversion rate, especially in the case of **2**, bearing eight flexible fluorenylmethyl groups.

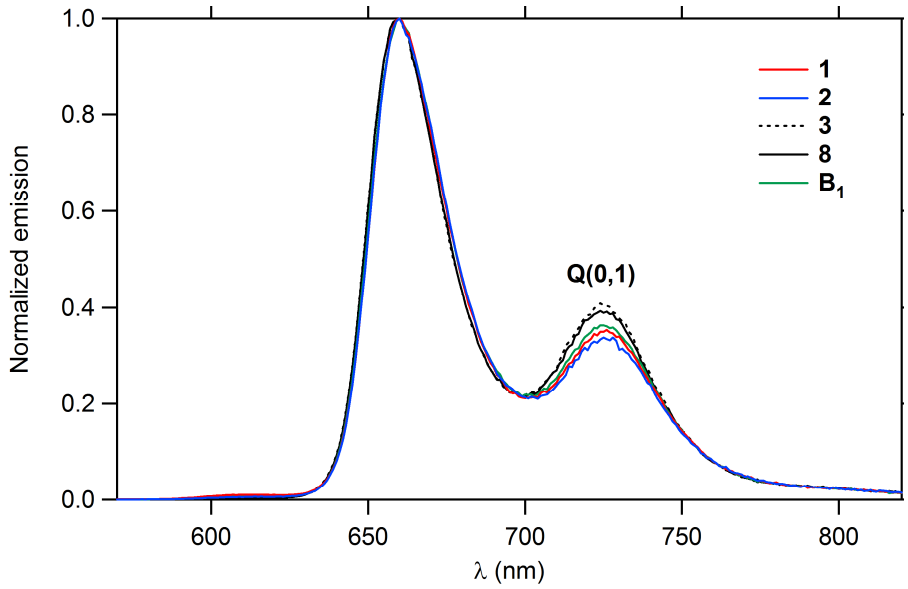

Figure 3. The normalized emission (em) spectra of new dendrimers **1**, **2** and reference compounds **TFPBu (3)**, **8** and $\mathbf{B_1}$ in CH_2Cl_2.

Photophysical properties of the model compounds 4 and 5

The emission spectra of **4** and **5** were measured in CH_2Cl_2 and their quantum yield were derived (Table 1). Considering the significant overlap between model donor emission and model acceptor absorption, the energy transfer (ET) from the donor fluorenyl dendrons toward the acceptor porphyrin central core in dendrimers **1-2** is possible. Figure 4 shows the emission spectra of isolated donors **4** and **5** (dashed lines) and the UV-visible absorption spectrum of the tetraalkynylporphyrin acceptor **8** (solid line). The absorption band of the ethynylfluorene moiety of **8** appears in UV region at 292 nm, whereas the maximum of the intense Soret band is at 428 nm, and the four Q-bands range at 520-650 nm (corresponding photophysical data are listed in Table 1). When the conjugated **4** was excited at 410 nm, a broad emission band in the region of 410-700 nm is observed. This emission band overlaps with the Soret and Q absorption bands of **8** (red hatched area), allowing in principle ET from dendron **4** towards the porphyrin core. Similarly, upon excitation of **5** at 274 nm, a narrow emission band has a partial overlap with the absorption spectrum of **8** (blue hatched area), which means that ET is also possible in this case (Figure 4).

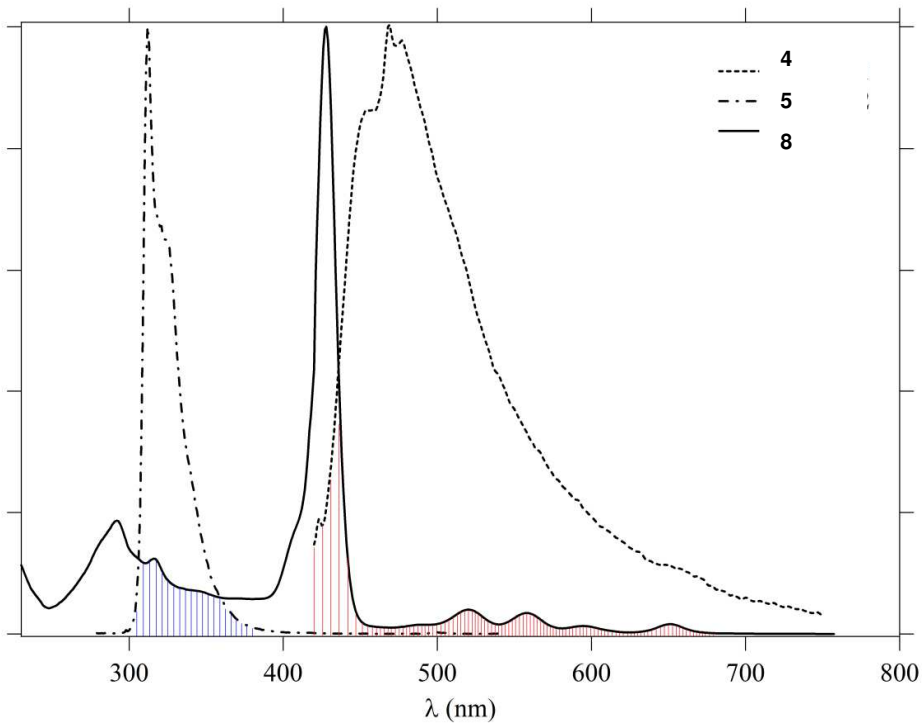

Figure 4. Overlaps between the emission spectrum of Model **4**, considered as the energy donor, and the absorption spectrum of porphyrin **8**, considered as the energy acceptor (red hatched area), and between the emission spectrum of Model **5** and the absorption spectrum of **8** (blue hatched area) in CH_2Cl_2.

Notably, the conjugated dendron Model **4** has a much lower quantum yield than the unconjugated Model **5**, presenting values close to these traditionally found for fluorenyl derivatives.[8] Quite likely, an efficient non-radiative quenching process is taking place in the former compound.

Energy transfer from the fluorene units to the porphyrin core in Dendrimers 1 and 2

After excitation in dendron absorption region (300 nm), the *conjugated* dendrimer **1** exhibits exclusively a red emission from porphyrin core as shown in Figure 5, which means that the ET efficiency is close to 100%. The broad emission band from conjugated peripheral dendrons (modelled by **4**) is completely quenched in the ET process, so that the red emission from the porphyrin core is exclusively seen, likewise to what had been previously observed for $\mathbf{B_0}$ and $\mathbf{B_1}$[11] For the dendrimer **2**, which has *non-conjugated* dendrons (modelled by **5**), the strong blue dendron emission is not totally quenched, and a very weak dendron emission band appears at 322 nm in addition to the red porphyrin emission. This dual emission suggests that ET from dendrons to **TFP** core is slightly less efficient than for **1,** but still near 100%. Additional data confirm the high efficiency of the ET process: i) the fluorescence quantum yields upon excitation in the dendron absorption band at 300 nm are exactly the same than upon excitation at the Soret band at 430 nm (17% for dendrimer **1** and 12% for dendrimer **2**), and ii) the excitation spectra of **1** and **2** closely resemble the corresponding absorption spectra (see Fig. S3, ESI). The maximum emission at 322 nm indicates that this residual emission comes from the non-conjugated pending fluorenyls (*i.e.* the flexible antenna, see Scheme 2), and not from the conjugated part of the dendrons (which belong to the extended **TFP** platform). To conclude, the ET is efficient in both cases, in relation with a good overlap between the emission spectrum of the dendron donors and the absorption spectrum of the **TFP** acceptor (see hatched areas in Figure 4).

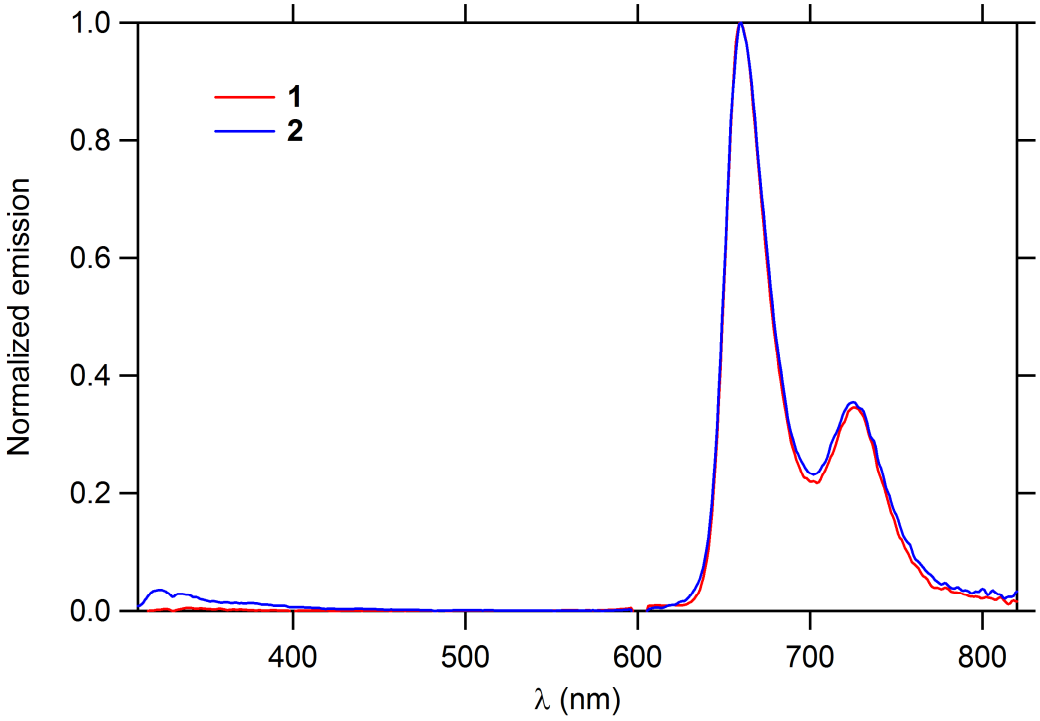

Figure 5. The normalized emission spectra of **1** and **2** upon excitation at the dendron band at 300 nm.

Two-photon absorption

Based on the fact that high two-photon absorption (2PA) cross-sections had previously been measured for $\mathbf{B_0}$ and $\mathbf{B_1}$[11] and other dendrimers possessing as well sixteen fluorenyl *antennae*,[10] we next turned our attention to the non-linear optical properties of **1** and **2**. Taking advantage of the good fluorescence of these **TFP**-cored dendrimers, their TPA cross-sections (σ_2) were determined by investigating their two-photon excited fluorescence (TPEF) in dichloromethane. Measurements were performed with 10^{-4} M solutions, using a mode-locked Ti:sapphire laser delivering femtosecond pulses, following the experimental protocol described by Xu and Webb.[31] A fully quadratic dependence of the fluorescence intensity on the excitation power was observed for each sample at all the wavelengths of the spectra shown in Figure 6, indicating that the cross-sections determined are only due to 2PA. The shape of these curves reveals the interest of limiting the red-shift of the lowest absorption (Q bands) in the higher generation dendrimers in order to be able to benefit of a pure two-photon excitation at highest energy, corresponding also to a better 2PA cross-section.

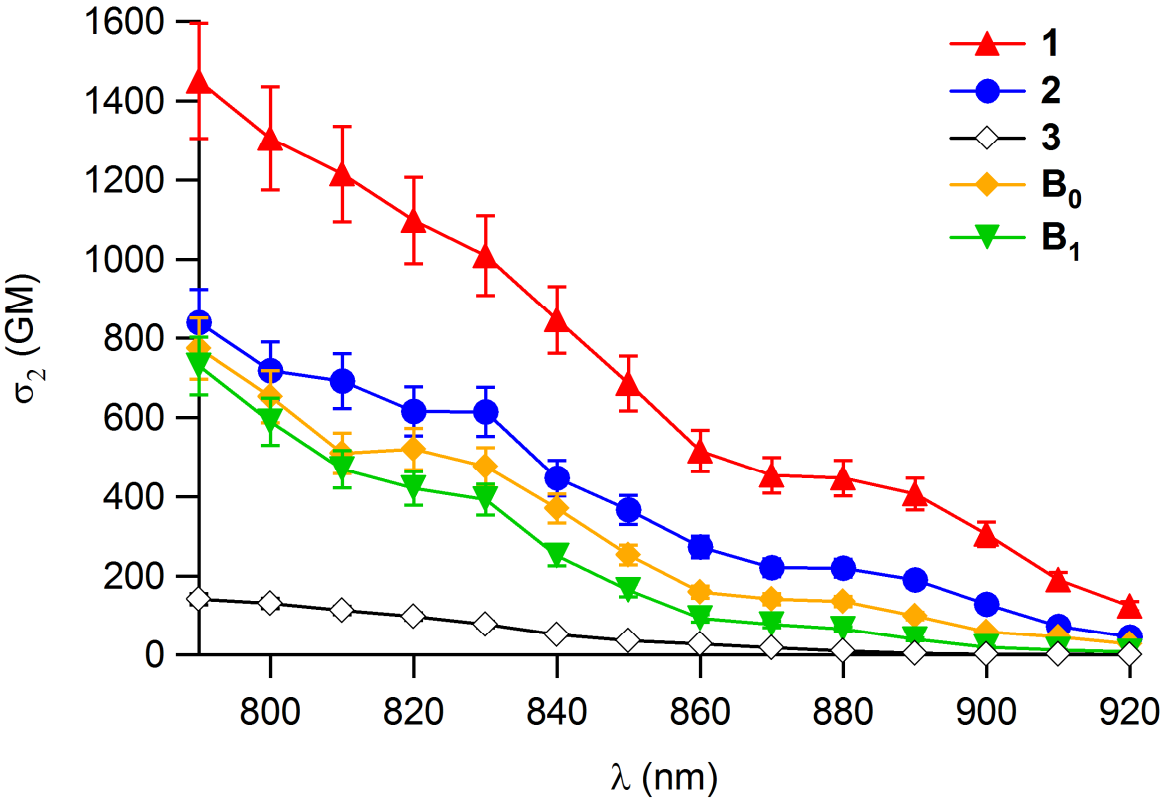

Figure 6. Two-photon absorption spectra of **1**, **2**, **TFPBu** (**3**), $\mathbf{B_0}$ and $\mathbf{B_1}$ in CH_2Cl_2.

An obvious increase of σ_2 values was observed for both new dendrimers **1** and **2** when compared to those of reference **TFPBu** (140 GM at 790 nm). Connection of dendron precursors **6** and **7** to the **TFP** core results in a strong improvement of the 2PA properties, up to a ten-fold increase of the 2PA cross sections in the case of **1** bearing rigid dendrons. The comparison between **1** and **2** clearly reveals the determining (positive) role of the conjugated spacer in **1** on 2PA cross-sections. Logically, these dendrons will also contribute to enhance the two-photon brightness ($\Phi_{fl} \cdot \sigma_2^{max}$), which evolves from 25 GM for **TFPBu** to 247 GM and 101 GM for **1** and **2**, respectively (Table 2).

Table 2. Two-Photon Absorption and Brightness Properties of dendrimers **1**, **2**, **TFPBu** and related reference compounds **TPP**, $\mathbf{B_0}$ and $\mathbf{B_1}$ in CH_2Cl_2.

Compound	λ_{2PA}^{max} /nm	σ_2^{max} /GM[a]	$\Phi_{fl} \cdot \sigma_2^{max}$ /GM[b]	Two-photon brightness enhancement factor [c]
1	**790**	**1450**	**247**	**190**

2	790	840	101	78
TFPBu (3)	790	140	25	19
TPP	790	12[d]	1.3	1
B_0	790	770	177	136
B_1	790	730	161	124

[a] Intrinsic TPA cross-sections measured in 10^{-4} M dichloromethane solutions by TPEF in the femtosecond regime;

[b] Maximum two-photon brightness in dichloromethane.

[c] Enhancement factor: $\Phi_{fl} \bullet \sigma_2^{max}$ of the compounds normalized to that of **TPP**.

[d] Data from reference.[32]

Comparison with the known dendrimers $\mathbf{B_0}$ or $\mathbf{B_1}$ is quite informative.[11] Thus, dendrimer **2** exhibits a 2PA cross-section similar to that of $\mathbf{B_0}$ (slightly higher, but within the error margin for the maximum value at 790 nm) and significantly larger than that of $\mathbf{B_1}$, in spite of the extended dendrimeric structure of the latter, in line with the determining role of the four conjugated fluorenyl ethynylfluorenyl arms at the *meso*-positions for 2PA. In contrast, dendrimer **1** exhibits 2PA cross-sections more than twice as large as those of $\mathbf{B_0}$ or $\mathbf{B_1}$, evidencing the additional positive effect of electronic conjugation within the dendrons on 2PA. Due to its lower fluorescence quantum yield relative to $\mathbf{B_0}$ or $\mathbf{B_1}$, **2** also exhibits lower two-photon brightness, whereas **1** is the brightest compound of these series (Table 2). This comparison clearly indicates that the enhancement of the 2PA cross-section observed for **1** actually results both from the increased number of fluorenyl units (one fluorenyl unit composing the connector) in each dendron but also from the conjugated (rigid) structure of the ***C_2* connector** in **1** which boosts 2PA more than the flexible and non-conjugated ***C_3* connector** in **2** (Scheme 2).

Table 3. Oxygen sensitization properties of dendrimers **1**, **2** and related reference compounds **TPP**, **TFPBu**, $\mathbf{B_0}$ and $\mathbf{B_1}$.

Compound	Φ_Δ [a]	$\Phi_\Delta \cdot \sigma_2^{max}$/GM [b]	**Two-photon excited oxygen sensitization enhancement factor (δ_{O2})** [c]
1	**0.46**	**667**	**93**

2	0.40	336	47
TFPBu (3)	0.64	90	13
TPP	0.60	7.2	1
B_0	0.62	477	66
B_1	0.61	445	62

[a] Singlet oxygen production quantum yield determined relative to **TPP** in dichloromethane (Φ_Δ[TPP] = 0.60).

[b] $\Phi_\Delta \cdot \sigma_2^{max}$: Figure of merit of the two-photon excited singlet oxygen production in dichloromethane.

[c] Enhancement factor: $\Phi_\Delta \cdot \sigma_2^{max}$ of the compound normalized to that of **TPP**.

Oxygen sensitization

We also wondered about the oxygen-sensitizing capabilities of **1**-**2**, by comparing their quantum yields of singlet oxygen generation (Φ_Δ) with those of **TFPBu**, **B_0** and **B_1** (Table 3).[11] The two new dendrimers exhibit values lower than those of the related reference compounds, however they still exhibit significant values (40 to 46 %). Dendrimer **1** exhibits singlet oxygen quantum yields higher than those of flexible dendrimer **2**, presumably in relation with a lower internal conversion rate. The decrease of the singlet oxygen production is concomitant with a strong increase of the 2PA cross-sections compared to **TFPBu**. This counteracting behavior of Φ_Δ and σ_2^{max} leads *in fine* to stronger enhancements of the figure of merit of the two-photon excited oxygen sensitization ($\Phi_\Delta.\sigma_2^{max}$) relative to **TFPBu** (up to a seven-fold increase for dendrimer **1**). When comparing the two-photon excited oxygen sensitization properties of **1** and **2** with those of **B_0** or **B_1**, similar trends are observed than previously noticed for the two-photon brightness: **2** is less efficient than **B_0** or **B_1**, due to its lower singlet oxygen quantum yield, but **1** is more efficient than **B_0** or **B_1**, because its lower Φ_Δ is largely compensated by its much larger σ_2.

Conclusions

Two new *conjugated* and *non-conjugated meso*-tetrafluorenylporphyrin-cored dendrimers **1** and **2** have been synthesized and characterized. For these dendrimers the peripheral fluorenyl units are linked to the central **TFP** core by original **fluorene-based connectors** instead of the more classic 1,3,5-phenylene unit previously used in related compounds. Absorption, emission and TPEF studies on these dendrimers **1** and **2** reveal that their two-photon absorption cross-sections are largely enhanced compared to that of **TFPBu**, ultimately leading to a better two-photon brightness ($\Phi_{fl} \cdot \sigma_2^{max}$) and enlarged two-photon excited oxygen sensitization ($\Phi_{\Delta} . \sigma_2^{max}$). These results point to a minimal impact of the dendrons on the linear optical properties, mostly determined by the **TFP** core, but not on the nonlinear optical properties which are largely influenced by the peripheral arms. Based on the classical figures of merit, dendrimer **1**, outperforms the best first-generation dendrimer (**B_1**) previously developed in our group,[11, 12, 33] but also the best porphyrin-based photosensitizer identified so far (**B_0**) for 2PA oxygen sensitization among these series. Thus, this new rigid and conjugated **fluorenyl-based connector** introduced in **1** leads to higher performances than the 1,3,5-phenylene spacer. This connector ameliorates the electronic communication within the dendrimeric branches without affecting the relevant linear optical properties for fluorescence imaging and oxygen photosensitization. It is therefore very promising for applied developments related to 2PA-PDT, since it enables improving the two-photon absorption cross-section while permitting a good trade-off with other important photophysical properties essential for theranostic uses (*i.e.* the fluorescence and singlet oxygen quantum yields). This new connector should now be used in the future when designing dendrimers for combined oxygen photosensitization and two-photon fluorescence imaging. Work is in progress to improve the water-solubility and the biocompatibility of this system, by replacing the alkyl chains on the fluorene units with water-solubilizing groups, such as oligoethyleneglycol chains.

Experimental Section

General

Unless otherwise stated, all solvents used in reactions were distilled using common purification protocols,[34] except DMF and $^{i}Pr_2NH$ which were dried on molecular sieves (3 Å). Compounds were purified by chromatography on silica gel using different mixtures of eluents as specified. ^{1}H and ^{13}C NMR spectra were recorded on BRUKER Ascend 400 and 500 at 298 K. The chemical shifts (in ppm) are referenced to internal tetramethylsilane. High-resolution mass spectra were recorded on different spectrometers: a Bruker MicrOTOF-Q II, a Thermo Fisher Scientific Q-Exactive in ESI positive mode and a Bruker Ultraflex III MALDI Spectrometer at CRMPO (centre regional de mesures physiques de l'Ouest) in Rennes. Reagents were purchased from commercial suppliers and used as received. Compounds 2-ethynyl-9,9-dibutyl-fluorene (**12**),[18,19] (9,9-dibutyl-fluorene-2-yl)carbaldehyde (**14**)[7] and 9,9-dibutyl-7-((trimethylsilyl)ethynyl)-fluorene-2-carboxaldehyde (**18**)[24] were synthesized as described earlier.

Synthesis of the organic precursors

2-Bromo-9-(dibromomethylene)-9H-fluorene (11a). In a Schlenk tube, 2-bromo-fluoren-9-one (**10**) (1.0 g, 3.9 mmol, 1 equiv) and PPh_3 (4.05 g, 15.4 mmol, 4 equiv) were dissolved in distilled and degassed CH_2Cl_2 under argon. The mixture was cooled to 0 °C in an ice-water bath. Then, CBr_4 (5.12 g, 15.4 mmol, 4 equiv) was added under argon. The mixture was stirred overnight at 20 °C. After evaporation of the volatiles, residue was further purified by silica chromatography using petroleum ether as eluent. The title compound was isolated as a yellow powder (1.17 g, 73% yield). ^{1}H NMR (400 MHz, $CDCl_3$): δ = 8.77 (s, 1H), 8.61 (d, 1H, J = 8.0 Hz), 7.66 (d, 1H, J = 8.0 Hz), 7.55 (s, 2H), 7.43 (t, 1H, J = 8.0 Hz), 7.34 (t, 1H, J = 8.0 Hz). ^{13}C NMR (100 MHz, $CDCl_3$): δ = 139.6, 139.4, 138.5, 137.8, 132.2, 129.6, 129.0, 127.7, 126.0, 121.0, 120.7, 119.6, 93.0, 92.3.

9-(Dibromomethylene)-9H-fluorene (11b). In a Schlenk tube, a mixture of commercial CBr_4 (368 mg, 1.1 mmol, 2 equiv) and PPh_3 (291 mg, 1.1 mmol, 2 equiv) were stirred in distilled and degassed CH_2Cl_2 (2 mL) at 35 ^{o}C under argon until the color turned to orange. Then, in another Schlenk tube, commercial *9*-fluorenone (**9**; 100 mg, 0.55 mmol, 1 equiv) dissolved in

CH_2Cl_2 (3 mL) and was transferred dropwise into the first Schlenk tube. The mixture was stirred at 35 °C for 5 h under argon. After evaporation of the volatiles, residue was purified by silica chromatography using heptane as eluent. The title compound was isolated as a white powder (130 mg, 70% yield) and characterized by ^{1}H NMR.[35][(see ESI)] ^{1}H NMR (400 MHz, $CDCl_3$): δ = 8.61 (d, J = 7.6Hz, 2H), 7.68 (d, J = 8.0 Hz, 2H), 7.42 (t, J = 8.0 Hz, 2H), 7.31 (t, J = 8.0 Hz, 2H).

2,2'-(3-(9H-fluoren-9-ylidene)penta-1,4-diyne-1,5-diyl)bis(9,9-dibutyl-9H-fluorene) (4). In a Schlenk tube, a mixture of 9,9-dibutyl-2-ethynyl-fluorene (**12**) (113 mg, 0.4 mmol, 2.5 equiv), **11b** (50 mg, 0.15 mmol, 1 equiv), $Pd(PPh_3)_2Cl_2$ (16.8 mg, 0.04 mmol, 0.6% equiv) and CuI (2.4 mg, 0.04 mmol, 0.6% equiv) were stirred in DMF (1 mL) and ^{i}Pr$_2$NH (1 mL) was added under argon. The reaction mixture was degassed by freeze-pump-thaw twice and heated for 48 h at 95 °C. After evaporation of the volatiles, residue was further purified by silica chromatography using pentane as eluent. Orange crystals of the title compound were obtained (33 mg, 28% yield). ^{1}H NMR (400 MHz, $CDCl_3$): δ = 8.81 (d, J = 4.0 Hz, 2H, H_{Flu}), 7.78-7.66 (m, 10H, H_{Flu}), 7.43-7.33 (m, 10H, H_{Flu}), 2.08-1.98 (m, 8H, C$H_{2\text{-Bu}}$), 1.16-1.07 (m, 8H, C$H_{2\text{-Bu}}$), 0.74-0.59 (m, 24H, J = 8.0 Hz, CH_2 & C$H_{3\text{-Bu}}$). MS (MALDI-DCTB) for $C_{60}H_{58}$: m/z = 778.4510 $[M+H]^+$ (calcd: 778.45385).

2,2'-(3-(2-bromo-9H-fluoren-9-ylidene)penta-1,4-diyne-1,5-diyl)bis(9,9-dibutyl-9H-fluorene) (6). In a Schlenk tube, a mixture of 9,9-dibutyl-2-ethynyl-fluorene (**12**) (300 mg, 1.0 mmol, 2 equiv), **11a** (206 mg, 0.5 mmol, 1 equiv), $Pd(PPh_3)_2Cl_2$ (4.2 mg, 0.01 mmol, 0.6% equiv) and CuI (0.6 mg, 0.01 mmol, 0.6% equiv) were stirred in DMF (2 mL) and ^{i}Pr$_2$NH (2 mL) was added under argon. The reaction medium was degassed by freeze-pump-thaw twice and heated for 48 h at 95 °C. After evaporation of the volatiles, residue was further purified by silica chromatography using pentane as eluent. The title compound was obtained as an orange powder (340 mg, 79% yield). ^{1}H NMR (400 MHz, $CDCl_3$): δ = 9.14 (d, J = 1.6 Hz, 1H, H_{Flu}), 8.79 (d, J = 8.0 Hz, 1H, H_{Flu}), 7.79-7.66 (m, 8H, H_{Flu}), 7.60-7.52 (m, 3H, H_{Flu}), 7.43-7.35 (m, 8H, H_{Flu}), 2.13-1.96 (m, 8H, C$H_{2\text{-Bu}}$), 0.90-0.83 (m, 8H, C$H_{2\text{-Bu}}$), 0.73-0.54 (m, 20H, H_{Flu}, CH_2 & C$H_{3\text{-Bu}}$). ^{13}C NMR (100 MHz, $CDCl_3$): δ = 151.4, 151.2, 143.3, 142.8, 142.7, 140.4, 140.3, 139.5, 139.3, 139.0, 137.6, 131.9, 131.2, 131.1, 129.6, 128.9, 128.1, 128.0, 127.9, 127.2, 127.1, 126.5, 126.3, 125.7, 123.1, 123.0, 121.3, 120.9, 120.8, 120.7,

120.4, 120.1, 120.0, 119.9, 103.3, 100.2, 100.1, 89.2, 89.1, 59.7, 55.5, 55.3, 53.6, 40.4, 40.3, 29.8, 29.5, 23.3, 23.2, 14.0. HRMS-ESI for $C_{60}H_{57}Br$: m/z = 856.3636 $[M]^{+\cdot}$ (calcd: 856.36381).

(9,9-dibutyl-9H-fluoren-2-yl)methanol (15). In a Schlenk tube, (9,9-dibutyl-fluorene-2-yl)carbaldehyde (**14**; 3.0 g, 9.8 mmol, 1 equiv) was dissolved in EtOH (99.6%) under argon. The mixture was cooled to 0°C in an ice-water bath. Then $NaBH_4$ (444 mg, 11.8 mmol, 1.2 equiv) was added under argon. The system was first stirred for 1 h at 0 °C, then for another 2 h at 20 °C. The mixture was extracted 3 times with ethyl acetate then washed by brine. After evaporation of the volatiles, the residue was further purified by silica chromatography using CH_2Cl_2/heptane (1:1) as eluent. The title compound was isolated as white crystals (2.94 g, 97% yield) and characterized by ^{1}H NMR by comparison with its known dihexyl analogue.[36] ^{1}H NMR (400 MHz, $CDCl_3$): δ = 7.70-7.67 (m, 2H, H_{Flu}), 7.34-7.29 (m, 5H, H_{Flu}), 4.78 (d, J = 5.64 Hz, 2H, CH_2OH), 1.98-1.94 (m, 4H, C$H_{2\text{-Bu}}$), 1.68 (t, J = 5.84 Hz, 1H, CH_2OH), 1.12-1.03 (m, 4H, C$H_{2\text{-Bu}}$), 0.67 (t, J = 8.0 Hz, 6H, C$H_{3\text{-Bu}}$), 0.63-0.55 (m, 4H, C$H_{2\text{-Bu}}$).

2-(bromomethyl)-9,9-dibutyl-9H-fluorene (16). In a two-neck flask, a mixture of **15** (1.13 g, 3.7 mmol, 1 equiv) and PPh_3 (1.06 g, 4.0 mmol, 1.1 equiv) was dissolved in THF (20 mL) and cooled to 15 °C. Then, NBS (717 mg, 4.0 mmol, 1.1 equiv) was added. The reaction was stirred for additional 1 h and immediately quenched by cold water. The precipitate was dissolved in CH_2Cl_2. The organic extracts were collected, washed with brine and dried over anhydrous $MgSO_4$. After evaporation of the volatiles, residue was further purified by silica chromatography using CH_2Cl_2/hexane (1:5) as eluent. The title compound was isolated as white crystals (639 mg, 86% yield) and characterized by ^{1}H NMR by comparison with its known dihexyl analogue.[36] ^{1}H NMR (400 MHz, $CDCl_3$): δ = 7.71-7.65 (m, 2H, H_{Flu}), 7.38-7.28 (m, 5H, H_{Flu}), 4.62 (s, 2H, CH_2Br), 1.99-1.95 (m, 4H, C$H_{2\text{-Bu}}$), 1.13-1.04 (m, 4H, C$H_{2\text{-Bu}}$), 0.68 (t, J = 8.0 Hz, 6H, C$H_{3\text{-Bu}}$), 0.64-0.67 (m, 4H, C$H_{2\text{-Bu}}$).

2,2'-((9H-fluorene-9,9-diyl)bis(methylene))bis(9,9-dibutyl-9H-fluorene) (5): Commercial fluorene (**17a**; 26 mg, 0.16 mmol, 1 equiv) and Bu_4NBr (5.0 mg, 0.02 mmol, 10% equiv) were dissolved in DMSO (2 mL) and then NaOH (50% aq., 0.02 mL) was injected into the mixture. After the color turning to orange, compound **16** (127 mg, 0.35 mmol, 2.2 equiv) was added

and stirred at 20 °C for 2 h. The mixture was extracted with CH_2Cl_2 for 3 times, washed with saturated NaCl and dried over anhydrous $MgSO_4$. After evaporation of the volatiles, residue was further purified by silica chromatography using heptane as eluent. The title compound was isolated as yellow crystals (88 mg, 79% yield). ^{1}H NMR (300 MHz, $CDCl_3$): δ = 7.55-7.49 (m, 4H, H_{Flu}), 7.34-7.28 (m, 6H, H_{Flu}), 7.24-7.16 (m, 8H, H_{Flu}), 6.70 (d, J = 9.0 Hz, 2H, H_{Flu}), 6.55 (s, 2H, H_{Flu}), 3.52 (s, 4H, $CH_{2\text{- bridging, }}H_{b,b'}$), 1.81(m, 4H, $CH_{2\text{-Bu}}$), 1.58 (m, 4H, $CH_{2\text{-Bu}}$), 1.06-0.93 (m, 8H, $CH_{2\text{-Bu}}$), 0.70-0.62 (m, 12H, $CH_{3\text{-Bu}}$), 0.42-0.17 (m, 8H, $CH_{2\text{-Bu}}$). HRMS-ESI for $C_{57}H_{62}$: m/z = 746.4849 $[M]^{+\cdot}$ (calcd: 746.4846); $C_{57}H_{63}$: m/z = 747.4925 $[M+H]^{+\cdot}$ (calcd: 747.49243);

2,2'-((2-bromo-9H-fluorene-9,9-diyl)bis(methylene))bis(9,9-dibutyl-9H-fluorene) (7): Commercial 2-bromofluorene (**17b**; 186 mg, 0.76 mmol, 1 equiv) and Bu_4NBr (24.4 mg, 0.076 mmol, 10% equiv) were dissolved in DMSO (6 mL) and then NaOH (50% aq., 0.05 mL) was injected into the system. After the color turning to orange, compound **16** (619 mg, 1.67 mmol, 2.2 equiv) was added and stirred at 20 °C for 1 h. The mixture was extracted with CH_2Cl_2 for 3 times, washed with brine and dried over anhydrous $MgSO_4$. After evaporation of the volatiles, the residue was further purified by silica chromatography using heptane as eluent. The title compound was isolated as a white powder (480 mg, 77% yield). ^{1}H NMR (400 MHz, CD_2Cl_2): δ = 7.88 (d, J^4 = 1.6 Hz, 1H, H_{Flu}), 7.67 (d, J = 7.6 Hz, 1H, H_{Flu}), 7.51-7.49 (m, 2H, H_{Flu}), 7.40 (t, J = 8.0 Hz, 1H, H_{Flu}), 7.32-7.29 (m, 2H, H_{Flu}), 7.24-7.16 (m, 10H, H_{Flu}), 6.64 (d, J = 5.8 Hz, 2H, H_{Flu}), 6.58 (s, 2H, H_{Flu}), 3.62-3.51 (m, 4H, $CH_{2\text{- bridging, }}H_{b,b'}$), 1.83-1.74 (m, 4H, $CH_{2\text{-Bu}}$), 1.66-1.57 (m, 4H, $CH_{2\text{-Bu}}$), 1.09-0.93 (m, 8H, $CH_{2\text{-Bu}}$), 0.63 (t, J = 7.32 Hz, 12H, $CH_{3\text{-Bu}}$), 0.31-0.11 (m, 8H, $CH_{2\text{-Bu}}$). ^{13}C NMR (100 MHz, CD_2Cl_2): δ = 151.2, 151.1, 150.1, 148.4, 141.5, 140.8, 140.7, 139.5, 136.3, 130.7, 129.3, 128.5, 127.9, 127.3, 127.1, 127.0, 125.4, 125.0, 121.3, 120.6, 120.1, 119.7, 118.7, 58.6, 55.0, 46.5, 40.7, 40.6, 30.3, 26.4, 26.3, 14.3, 14.2. HRMS-ESI for $C_{57}H_{61}Br$: m/z = 847.3850 $[M+Na]^+$ (calcd: 847.38488); m/z = 825.4040 $[M+H]^+$ (calcd: 825.40294). Anal. Calcd. (%) for $C_{57}H_{61}Br$: C 82.88; H 7.44. Found: C 82.71; H 7.66.

5,10,15,20-Tetrakis(9,9-dibutyl-7-ethynyl-9H-fluoren-2-yl)porphyrin (8): In a two-neck flask, a mixture of previously prepared 9,9-dibutyl-7-((trimethylsilyl)ethynyl)-fluorene-2-carboxaldehyde (**18**; 689 mg, 1.7 mmol, 1 equiv) and pyrrole (0.17 mL, 1.7 mmol, 1 equiv)

were dissolved in dried chloroform (200 mL) under argon. After degassing the mixture with argon bubbling for 30 min, BF_3•OEt_2 (0.05 mL, 0.4 mmol, 0.25 equiv) was injected and the reaction was stirred in dark for 3 h under argon at room temperature. Then oxidant *p*-chloranil (315 mg, 1.28 mmol, 0.75 equiv) was added, and the reaction was heated at 60 °C for another 2 h without any protection. After cooling the reaction to room temperature, NEt_3 (2 mL) was injected and then stirring was kept for several minutes. After evaporation of the volatiles, purification was done by silica chromatography using [CH_2Cl_2/heptane (1:4)] mixture as eluent; the porphyrin **19** was collected as a red powder. The crude porphyrin **19** was then deprotected by K_2CO_3 (470 mg, 3.4 mmol, 8 equiv) in a mixed solvents CH_2Cl_2/THF/MeOH (3:1:1) at 60°C, overnight. At last, the title tetra-alkynyl porphyrin was isolated by silica chromatography using a CH_2Cl_2/heptane (1:4) mixture as eluent. The overall yield is 28% for these two steps. ^{1}H NMR (400 MHz, $CDCl_3$): δ = 8.90 (s, 8H, $H_{\beta\text{-pyr}}$), 8.25-8.19 (m, 8H, H_{Flu}), 8.07 (d, 4H, J = 7.3 Hz, H_{Flu}), 7.91 (d, 4H, J = 7.8 Hz, H_{Flu}), 7.63 (m, 8H, J = 8.0 Hz, H_{Flu}), 3.21 (s, 4H, C≡C*H*), 2.13 (t, 16H, J = 6.9 Hz, C$H_{2\text{-Bu}}$), 1.21-1.14 (m, 16H, C$H_{2\text{-Bu}}$), 0.92-0.83 (m, 16H, C$H_{2\text{-Bu}}$), 0.79-0.73 (m, 24H, C$H_{3\text{-Bu}}$), -2.60 (s, 2H, N*H*). ^{13}C NMR (100 MHz, $CDCl_3$): δ = 151.4, 149.7, 141.9, 141.7, 140.1, 133.9, 131.6, 129.5, 126.9, 120.8, 120.2, 118.4, 88.6, 84.9, 55.5, 40.4, 26.5, 23.3, 14.1. MS (Maldi-DCTB) for $C_{112}H_{110}N_4$: m/z = 1510.869 [$M^{+\bullet}$] (calcd: 1510.8725). Anal. Calcd. (%) for $C_{112}H_{110}N_4$.EtOH: C, 87.87; H, 7.50; N, 3.60. Found: C, 87.89; H, 7.59; N, 3.49.

Conjugated Porphyrin-based Dendrimer (1): In a Schlenk tube, the dendron precursor **6** (100 mg, 0.12 mmol, 4.5 equiv), porphyrin **8** (39 mg, 0.03 mmol, 1 equiv), $Pd(PPh_3)_2Cl_2$ (4.2 mg, 0.01 mmol, 0.6% equiv) and CuI (0.6 mg, 0.01 mmol, 0.6% equiv) were stirred in DMF (2 mL) under argon. Subsequently, degassed ^{i}Pr_2NH (2 mL) was added and the reaction medium was degassed by freeze-pump-thaw twice and heated for 72 h at 95 °C. After evaporation of the volatiles, residue was purified by silica chromatography using petroleum ether/THF (30:1) as eluent. The title porphyrin-based dendrimer was isolated as a dark violet powder (26 mg, 22% yield). ^{1}H NMR (400 MHz, $CDCl_3$): δ = 9.23 (t, J = 8.8 Hz, 4H, H_{Flu}), 8.97 (m, 8H, $H_{\beta\text{-pyr}}$), 8.87-8.83 (m, 4H, H_{Flu}), 8.67-8.50 (m, 4H, H_{Flu}), 8.28 (m, 8H, H_{Flu}), 8.11-8.09 (m, 4H, H_{Flu}), 7.99-7.88 (m, 10H, H_{Flu}), 7.79-7.61 (m, 38H, H_{Flu}), 7.44-7.34 (m,

28H, H_{Flu}), 2.27-1.97 (m, 48H, C$H_{2\text{-Bu}}$), 1.19-1.06 (m, 48H, C$H_{2\text{-Bu}}$), 0.78-0.58 (m, 110H, CH_2 & C$H_{2\text{-Bu}}$), -2.53 (s, 2H, N*H*). ^{13}C NMR (100 MHz, $CDCl_3$): δ = 151.5, 151.4, 151.3, 151.2, 140.4, 140.3, 140.0, 139.8, 138.3, 137.8, 131.2, 131.1, 129.7, 129.4, 128.0, 127.2, 126.5, 123.1, 121.1, 121.0, 120.5, 120.4, 120.2, 120.1, 120.0, 55.4, 55.3, 40.4, 26.1, 23.2, 14.1, 14.0. MS (ES-CH_2Cl_2) for $C_{352}H_{336}N_4$: m/z = 2309.3104 $[M]^{2+}$ (calcd: 2309.3202); MS (MALDI) for $C_{352}H_{335}N_4$: m/z = 4617.693 $[M+H]^+$ (calcd: 4617.63313). Anal. Calcd. (%) for $C_{352}H_{336}N_4 \cdot 4CH_2Cl_2$: C, 86.14; H, 6.98; N, 1.14. Found: C, 86.39; H, 7.09; N, 1.26.

Non-conjugated Porphyrin-based Dendrimer (2): In a Schlenk tube, the Dendron precursor **7** (100 mg, 0.14 mmol, 4.5 equiv), the porphyrin **8** (45 mg, 0.03 mmol, 1 equiv), $Pd(PPh_3)_2Cl_2$ (4.2 mg, 0.01 mmol, 0.6% equiv) and CuI (0.6 mg, 0.01 mmol, 0.6% equiv) were stirred in DMF (2 mL) under argon. Subsequently, degassed $^{i}Pr_2NH$ (2 mL) was added and the reaction medium was degassed by freeze-pump-thaw twice and heated for 114 h at 95 ^{o}C. After evaporation of the volatiles, residue was purified by silica chromatography using petroleum ether/THF (30:1) as eluent. The title porphyrin-based dendrimer was isolated as a dark violet powder (38 mg, 29% yield). ^{1}H NMR (400 MHz, CD_2Cl_2): δ = 9.00 (s, 8H, $H_{\beta\text{-pyr}}$), 8.31-7.96 (m, 22H, H_{Flu}), 7.77-7.68 (m, 12H, H_{Flu}), 7.50-6.97 (m, 60H, H_{Flu}), 6.71-6.63 (m, 14H, H_{Flu}), 3.63 (s, 16H, C$H_{2\text{-bridging}}$), 2.24-1.64 (m, 48H, C$H_{2\text{-Bu}}$), 1.09-0.75 (m, 72H, C$H_{3\text{-Bu}}$), 0.64-0.23 (m, 96H, C$H_{2\text{-Bu}}$), -2.59 (s, 2H, N*H*). ^{13}C NMR (100 MHz, CD_2Cl_2): δ = 151.6, 150.6, 149.6, 149.5, 141.4 141.1, 140.0, 138.8, 136.0, 132.1, 130.9, 130.8 , 128.7, 126.5, 124.9, 124.5, 122.7 , 121.1, 119.4, 119.2, 118.1, 54.5, 45.9, 40.3, 40.1, 29.7, 25.7, 23.1, 22.7, 13,7, 13.6. Anal. Calcd. (%) for $C_{340}H_{350}N_4 \cdot 3CH_2Cl_2$: C, 86.78; H, 7.54; N, 1.18. Found: C, 87.39; H, 7.90; N, 1.01.

Spectroscopic Measurements

All photophysical properties have been performed with freshly-prepared air-equilibrated solutions at room temperature (298 K). UV-Vis absorption spectra were recorded on a Jasco V-570 spectrophotometer. Steady-state fluorescence measurements were performed on dilute solutions (*ca.* 10^{-6} M, optical density < 0.1) contained in standard 1 cm quartz cuvettes using an Edinburgh Instrument (FLS920) spectrometer in photon-counting mode. Fully corrected emission spectra were

obtained, for each compound, after excitation at the wavelength of the absorption maximum, with $A_{\lambda ex}$ < 0.1 to minimize internal absorption.

Measurements of singlet oxygen quantum yield (Φ_Δ)

Measurements were performed on a Fluorolog-3 (Horiba Jobin Yvon), using a 450 W Xenon lamp. The emission at 1272 nm was detected using a liquid nitrogen-cooled Ge-detector model (EO-817L, North Coast Scientific Co). Singlet oxygen quantum yields Φ_Δ were determined in dichloromethane solutions, using tetraphenylporphyrin (TPP) in dichloromethane as reference solution (Φ_Δ [TPP] = 0.60) and were estimated from $^1O_2$ luminescence at 1272 nm.

Two-Photon Absorption Experiments

To span the 790-920 nm range, a Nd:YLF-pumped Ti:sapphire oscillator (Chameleon Ultra, Coherent) was used generating 140 fs pulses at a 80 MHz rate. The excitation power is controlled using neutral density filters of varying optical density mounted in a computer-controlled filter wheel. After five-fold expansion through two achromatic doublets, the laser beam is focused by a microscope objective (10x, NA 0.25, Olympus, Japan) into a standard 1 cm absorption cuvette containing the sample. The applied average laser power arriving at the sample is typically between 0.5 and 40 mW, leading to a time-averaged light flux in the focal volume on the order of 0.1–10 mW/mm^2. The fluorescence from the sample is collected in epifluorescence mode, through the microscope objective, and reflected by a dichroic mirror (Chroma Technology Corporation, USA; ''red'' filter set: 780dxcrr). This makes it possible to avoid the inner filter effects related to the high dye concentrations used (10^{-4} M) by focusing the laser near the cuvette window. Residual excitation light is removed using a barrier filter (Chroma Technology; ''red'': e750sp–2p). The fluorescence is coupled into a 600 µm multimode fiber by an achromatic doublet. The fiber is connected to a compact CCD-based spectrometer (BTC112-E, B&WTek, USA), which measures the two-photon excited emission spectrum. The emission spectra are corrected for the wavelength-dependence of the detection efficiency using correction factors established through the measurement of reference compounds having known fluorescence emission spectra. Briefly, the set-up allows for the recording of corrected fluorescence emission spectra under multiphoton excitation at variable excitation power and wavelength. TPA cross sections (σ_2) were

determined from the two-photon excited fluorescence (TPEF) cross sections ($\sigma_2.\Phi_F$) and the fluorescence emission quantum yield (Φ_F). TPEF cross sections of 10^{-4} M dichloromethane solutions were measured relative to fluorescein in 0.01 M aqueous NaOH using the well-established method described by Xu and Webb[31] and the appropriate solvent-related refractive index corrections.[37] The quadratic dependence of the fluorescence intensity on the excitation power was checked for each sample and all wavelengths. The experimental uncertainty on the absolute cross-sections determined by this method has been estimated to be ± 10%.

Acknowledgments

The authors acknowledge the China Scholarship Council (CSC) for Ph.D. funding (X. Z) and "the Ministère de l'Enseignement Supérieur et de la Recherche Scientifique de Tunisie" for PhD funding (SBH). This project was supported by the departmental committees CD35 and CD85 of the "Ligue contre le Cancer du Grand-Ouest". We also thank Guillaume Clermont (ISM) for his help with the two-photon and singlet oxygen measurements.

References

[1] K. Szacilowski, *Chem. Rev.* **2008**, *108*, 3481.

[2] M. R. Wasielewski, *J. Org. Chem.* **2006**, *71*, 5051.

[3] L. B. Josefsen, R. W. Boyle, *Theranostics* **2012**, *2*, 916.

[4] M. Pawlicki, H. A. Collins, R. G. Denning, H. L. Anderson, *Angew. Chem. Int. Ed.* **2009**, *48*, 3244.

[5] J. Bhaumik, A. K. Mittal, A. Banerjee, Y. Chisti, U. C. Banerjee, *Nano Res.* **2015**, *8*, 1373.

[6] P. Prabhu, V. Patravale, *J. Biomed. Nanotechnol.* **2012**, *8*, 859.

[7] F. Bolze, S. Jenni, A. Sour, V. Heitz, *Chem. Commun.* **2017**, *53*, 12857.

[8] O. Mongin, V. Hugues, M. Blanchard-Desce, A. Merhi, S. Drouet, D. Yao, C. Paul-Roth, *Chem. Phys. Lett.* **2015**, *625*, 151.

[9] S. Drouet, C. O. Paul-Roth, G. Simonneaux, *Tetrahedron* **2009**, *65*, 2975.

[10] S. Drouet, C. O. Paul-Roth, *Tetrahedron* **2009**, *65*, 10693.

[11] D. Yao, X. Zhang, A. Triadon, N. Richy, O. Mongin, M. Blanchard-Desce, F. Paul, C. O. Paul-Roth, *Chem. Eur. J.* **2017**, *23*, 2635.

[12] D. Yao, X. Zhang, O. Mongin, F. Paul, C. O. Paul-Roth, *Chem. Eur. J.* **2016**, *22*, 5583.

[13] The δ_{O2} factor corresponds to the 2PA singlet oxygen production for a given compound (Φ_{Δ}•σ2max) normalized by that of **H_2TPP**.

[14] W. T. Borden, H. Iwamura, J. A. Berson, *Acc. Chem. Res.* **1994**, *27*, 109.

[15] J. S. Lindsey, K. A. Maccrum, J. S. Tyhonas, Y. Y. Chuang, *J. Org. Chem.* **1994**, *59*, 579.

[16] F. R. Li, K. X. Yang, J. S. Tyhonas, K. A. Maccrum, J. S. Lindsey, *Tetrahedron* **1997**, *53*, 12339.

[17] K. Sonogashira, Y. Tohda, N. Hagihara, *Tetrahedron Lett.* **1975**, *50*, 4467.

[18] A. Triadon, G. Grelaud, N. Richy, O. Mongin, G. J. Moxey, I. M. Dixon, X. Yang, G. Wang, A. Barlow, J. Rault-Berthelot, M. P. Cifuentes, M. G. Humphrey, F. Paul, *Organometallics* **2018**, *35*, 2245.

[19] F. Malvolti, C. Rouxel, A. Triadon, G. Grelaud, N. Richy, O. Mongin, M. Blanchard-Desce, L. Toupet, F. I. Abdul Razak, R. Stranger, M. Samoc, X. Yang, G. Wang, A. Barlow, M. P. Cifuentes, M. G. Humphrey, F. Paul, *Organometallics* **2015**, *34*, 5418.

[20] S. E. Kiruthika, P. T. Perumal, *Org. Lett.* **2014**, *16*, 484.

[21] C. Adachi, M. A. Baldo, M. E. Thompson, S. R. Forrest, *J. Appl. Phys.* **2001**, *90*, 5048.

[22] K. R. J. Thomas, J. T. Lin, C. Tsai, H. Lin, *Tetrahedron* **2006**, *62*, 3517.

[23] S. Abraham, G. P. T. Ganesh, S. Varughese, J. J. B. Deb, *ACS Appl. Mater. Interfaces* **2015**, *7*, 25424.

[24] X. Zhang, C. Paul-Roth, O. Mongin, F. Paul, *unpublished results*.

[25] C. O. Paul-Roth, G. Simonneaux, *C. R. Acad. Sci., Ser. IIb; Chim.* **2006**, *9*, 1277.

[26] C. O. Paul-Roth, G. Simonneaux, *Tetrahedron Lett.* **2006**, *47*, 3275.

[27] C. O. Paul-Roth, J. A. G. Williams, J. Letessier, G. Simonneaux, *Tetrahedron Lett.* **2007**, *48*, 4317.

[28] O. Mongin, L. Porrès, M. Charlot, C. Katan, M. Blanchard-Desce, *Chem. Eur. J.* **2007**, *13*, 1481.

[29] N. I. Nijegorodov, W. S. Downey, *J. Phys. Chem.* **1994**, *98*, 5639.

[30] P. G. Seybold, M. Gouterman, *J. Mol. Spectroscopy* **1969**, *31*, 1.

[31] C. Xu, W. W. Webb, *J. Opt. Soc. Am. B* **1996**, *13*, 481.

[32] N. S. Makarov, M. Drobizhev, A. Rebane, *Opt. Express* **2008**, *16*, 4029.

[33] X. Zhang, S. Abid, L. Shi, O. Mongin, M. Blanchard-Desce, F. Paul, C. O. Paul-Roth, *Dyes and Pigments* **2018**, *153*, 248.

[34] D. D. Perrin, W. L. F. Armarego, *Purification of Laboratory Chemicals*, 3rd ed., Pergamon Press, Oxford NY Beijing Frankfurt Sao-Paulo Sidney Tokyo Toronto, **1988**.

[35] G.-F. Zhang, M. P. Aldred, Z.-Q. Chen, T. Chen, X. Meng, M.-Q. Zhu, *RSC Adv.* **2015**, *5*, 1079.

[36] W.-S. Huang, C.-W. Lin, J. T. Lin, J.-H. Huang, C.-W. Chu, Y.-H. Wud, H.-C. Lin, *Organic Electronics* **2009**, *10*, 594.

[37] M. H. V. Werts, N. Nerambourg, D. Pélégry, Y. Le Grand, M. Blanchard-Desce, *Photochem. Photobiol. Sci.* **2005**, *4*, 531.